Design Methodology for the Frequency Shift Method of Islanding Prevention and Analysis of its Detection Capability

Pablo Sanchis[1], Luis Marroyo[1] and Javier Coloma[2]

- Authors organizational affiliation:

  [1]Department of Electrical and Electronic Engineering, Public University of Navarra, Pamplona, Spain

  [2]Photovoltaic Area, INGETEAM, Pamplona, Spain

- Corresponding author: Dr. Pablo Sanchis
  - Postal address:

    Edificio Los Pinos, Dpto. Ingenieria Electrica y Electronica

    Universidad Publica de Navarra, Campus Arrosadia

    31006 Pamplona, Spain
  - Voice telephone number: +34 948 169613
  - Fax telephone number: +34 948 169884
  - email: pablo.sanchis@unavarra.es

ABSTRACT

Islanding protection is one of the most important sources of discrepancy in grid-connected photovoltaic systems. Even when islanding is not very likely to happen, regulations demand the photovoltaic inverters to implement effective protection methods. Due to its several advantages, the frequency shift method of islanding prevention, commonly known as Sandia Frequency Shift, is one of the most important active methods. This method implements a positive feedback of the frequency that tends to move it outside the trip limits in case of islanding. The method shows a very high detection capability, which depends on both the values of the method parameters and the characteristics of the load that remains in the same power section after islanding.

This paper develops a mathematical analysis of the Sandia Frequency Shift method and proposes a new methodology to design its parameters as a trade-off between the detection capability, which is evaluated as a function of the load characteristics, and the distortion that the method could introduce in the grid as a consequence of transitory frequency disturbances. The ability of this methodology to design the method parameters and achieve the highest detection capability is satisfactorily proved by means of both simulation and experimental results on a commercial photovoltaic inverter that implements the method once its parameters have been designed with the proposed methodology.

KEYWORDS

Grid-connected photovoltaic inverters; inverters; islanding; protection; photovoltaic power systems.

I. INTRODUCTION

The islanding condition is that situation in which a grid-connected photovoltaic inverter continues supplying the loads that are connected within its grid section after a mains disconnection. This can happen as a consequence of maintenance reasons, fault conditions like short-circuits, etc. Islanding can cause problems to the operation of the grid and other units within the power island. To a lesser extent it can also be hazardous for the maintenance staff.[1,2,3] Due to these reasons, photovoltaic inverters have to be protected against islanding,[4] even when its probability of occurrence is very low.[3,5-8]

The use of grid-connected photovoltaic systems is now increasing very fast. However, national and international regulations concerning islanding are still mostly under discussion. Actually, islanding protection is one of the most important sources of discrepancy.[4,5]

Several islanding detection techniques can be found in the literature.[1,2,4,5,9-26] They can be mainly classified in two groups: passive and active methods. The passive methods try to detect islanding by means of *observing* the evolution of the inverter output electrical variables.[2,4,5,9,13,14,16] On the other hand, the active methods disturb these variables as a way to detect islanding according to the system reaction.[1,2,4,9-26]

The most commonly used passive methods are the voltage and frequency monitoring methods. These methods monitor the output voltage rms-value and frequency, and activate the voltage and frequency relays when these magnitudes exceed the programmed limits. Since most standards and regulations demand protection relays, the voltage and frequency monitoring methods are commonly implemented in photovoltaic inverters.[27,28] Obviously, these methods do not provide detection if voltage and frequency lie inside the relays limits after islanding occurs.[4,5] Two other passive methods are sometimes suggested: voltage harmonic monitoring and phase jump detection. The first one monitors the harmonic content and disconnects the unit when a limit is exceeded.[2] The phase jump detection technique monitors the phase-shift between the inverter voltage and current, and activates the protection relays when the phase-shift

experiments a sudden change.[9] Both methods are not very used due to the difficulty of selecting the trip limits and their sensibility to noise sources and mains transients.

Due to the fact that passive methods cannot always guarantee detection,[2] active methods are proposed as an alternative to voltage and frequency monitoring, or more often as a support. There are mainly two types of active methods: those that are continuously disturbing the inverter output variables in order to measure some parameters and those that only start disturbing these variables when they notice that the variables have changed. The active frequency drift and impedance measurement methods belong to the first group, while the frequency shift, the voltage shift and the slide-mode frequency shift methods belong to the second one.

The active frequency drift generates a distorted current waveform in such a way that, in case of islanding, the frequency tends to move outside the trip limits.[2,10-12] When this method is implemented with a positive feedback, the islanding detection capability increases significantly.[2,11,13] However, the method has two important drawbacks. Firstly, this method is always injecting a distorted current in the mains, which is an important drawback shared by this kind of active methods that may result in flicker problems.[4] Secondly, some loads can compensate the frequency shift, thus reducing the islanding detection capability.[2,14-16]

The impedance measurement detection method introduces a periodic disturbance in the output current and then estimates the value of the impedance by measuring and averaging the voltage and current during the disturbance.[2,18] A change or a high value in the estimated impedance can be used to detect an island situation. One of the reasons that this method is important is that it is demanded by the regulations of Germany and other countries.[28] However, it has been shown in the literature that it is not a very effective method to detect islanding.[4,17,18] Firstly, the disturbance in the current has to be injected during a period of time short enough to distort as low as possible the grid.[17] The impedance is then very difficult to be accurately estimated from the voltage and current as they are measured during quite a short time. In addition, the choice of the impedance variation threshold value is not a small problem. Too high

values reduce the detection capability while too small values can lead to false detections. Finally, this method is highly ineffective in case of multiple inverters connected in the same power section.[4,17-20] The requirement of implementing the impedance measurement method in grid-connected photovoltaic inverters is now under discussion in most of the countries where regulations demand it. This can lead to a change in the present regulations.

The slide-mode frequency shift method controls the phase-shift between the inverter output current and voltage as a function of the measured frequency.[2,21-24] When an island occurs the frequency changes and the method increases or decreases the phase-shift in order to make the frequency drift toward values outside the trip limits. However, this method can be ineffective when the characteristics of the load supplied by the inverter interact with the method and the frequency stabilizes in a value inside the trip limits.[2,11,14] As a consequence, this method is not very used in photovoltaic inverters.

The voltage and frequency shift methods, commonly known as Sandia Voltage and Frequency Shift methods, try to unbalance these variables by means of a positive feedback of their measured values.[1,4,25] When an island appears, the mains does not fix the voltage and frequency anymore, and they move depending on the load. The voltage shift method moves the output current amplitude in the direction of the voltage variations thus trying to get the system out of the voltage relay limits. Although this method achieves a high islanding detection capability, it has two important drawbacks, which are the variability in the grid voltage rms-value and the required variations in the real power provided by the inverter.

The frequency shift method is based on the same philosophy as the voltage shift method. When a change in the frequency is detected, the method modifies the output current frequency in the same direction. In case of islanding, the method provokes a continuous drifting in the frequency until it gets out of the frequency relay limits. Unlike the voltage shift method, the frequency shift method does not require real power variation, and thus its effectiveness is considerably higher. Indeed, this method is considered to be one of the most effective islanding detection methods.[1,4,14,18,25] This high prevention capability, together with the fact that it does

not introduce a periodic disturbance on the mains, have led this method to be one of the most used methods in the detection of islanding situations in grid-connected photovoltaic systems. Likewise, this method is usually demanded or at least recommended by many regulations, such as those from the USA.[27,29]

In spite of the good properties of the frequency shift method, a lack has been observed in the literature concerning the design of the parameters of this method and the analysis of its detection capability as a function of the parameters choice.

This paper carries out a mathematical analysis of the frequency shift method and proposes a new methodology to design its parameters as a function of the islanding detection capability and the load characteristic parameters. After a short description of the method, the proposed methodology is developed to design the two main parameters of the method, which are the *frequency shift constant* and the *frequency shift limit*. The choice of the values for these parameters is proposed to be made according to the desired detection capability, the evaluation of which is made taking into account the load parameters such as the quality factor, the resonant frequency, the reactive power, etc. In addition, the distortion that the method could generate in the output current of the photovoltaic inverter when the grid is connected is also evaluated as an additional criterion to select the values for the method parameters. This distortion can appear as a consequence of frequency measurement errors, transient situations, etc. As a conclusion, the selection of the method parameters can then be made as a trade-off between a high detection capability and a low current distortion, once the detection capability has been evaluated as a function of the load characteristic parameters.

The ability of the proposed methodology to design the parameters of the frequency shift islanding detection method and achieve the highest detection capability is satisfactorily proved by means of both simulation and experimental results. These results are taken from a commercial photovoltaic inverter that implements the method once its parameters have been designed by means of the proposed methodology. As it will be shown, the results show that the islanding condition is virtually impossible to happen.

In short, this paper tries to contribute to the debate on the effectiveness of the islanding detection methods by showing the higher detection capability of the frequency shift method once its parameters have been designed by means of the proposed methodology.

II. DESCRIPTION OF THE ISLANDING SITUATION THROUGH *RLC* PARALLEL LOADS

II.1 The Islanding Maps and the Non-Detection Zones

Figure 1 illustrates the normal operation of a grid-connected photovoltaic system and a load that is within the same power section.[2,5] The photovoltaic system consists of a photovoltaic generator and an inverter. The load is a parallel *RLC* circuit that describes most of the loads that can be connected to a photovoltaic inverter in an island power section. The photovoltaic system is supplying the real and reactive powers P_{PV} and Q_{PV}, respectively, and the load is consuming the real and reactive powers P_C and Q_C, respectively. The real and reactive powers supplied by the mains, which are denoted ΔP and ΔQ, respectively, are therefore:

$$\Delta P = P_C - P_{PV} \tag{1}$$

$$\Delta Q = Q_C - Q_{PV} \tag{2}$$

The real and reactive powers P_C and Q_C consumed by the *RLC* load are:

$$P_C = V_g \frac{V_g}{R} \tag{3}$$

$$Q_C = V_g^2 \left(\frac{1}{\omega_g L} - \omega_g C \right) \tag{4}$$

where V_g and ω_g are the mains rms-voltage and angular frequency before islanding occurs, and R, L and C are the resistive, inductive and capacitive components of the load. The reactive power Q_{PV} is usually zero or very close to zero since photovoltaic inverters are controlled to achieve a unity power factor.

The islanding situation is usually analysed by means of the so-called Islanding Maps and Non-Detection Zones (NDZ).[2,5] The Islanding Maps are bi-dimensional maps defined by ΔP and ΔQ. The Non-Detection Zone is the area of these maps in which islanding occurs. Its size is used to evaluate the detection capability of an islanding prevention method. The variation that appears in the voltage and frequency when the mains is disconnected depends on the magnitude of ΔP and ΔQ. As ΔP and ΔQ get smaller, the variations in the voltage and frequency get less significant and then the islanding detection becomes more difficult.

II.2 Influence of the quality factor and the resonant frequency

Once ΔP and ΔQ are provided, the values for R, L and C can be calculated. The value for the resistance R can be easily obtained from Equations (1) and (3):

$$R = \frac{V_g^2}{\Delta P + P_{PV}} \tag{5}$$

In order to determine the values of L and C, the load quality factor (Q_f) is used as an additional parameter besides ΔQ. Its expression at the angular resonant frequency (ω_r) is:

$$Q_f = R\sqrt{\frac{C}{L}} = \frac{R}{\omega_r L} \quad \text{with} \quad \omega_r = \frac{1}{\sqrt{LC}} \tag{6}$$

Then, for a given Q_f the expressions for L and C are:

$$L = \frac{-\Delta Q R^2 + R\sqrt{\Delta Q^2 R^2 + 4V_g^4 Q_f^2}}{2\omega_g V_g^2 Q_f^2} \qquad C = \frac{Q_f^2}{R^2} L \tag{7}$$

When islanding occurs, the frequency of the power section moves to the load resonant frequency. The importance of the quality factor in the islanding detection lies in the fact that represents somehow the strength of the load to make the system move to its resonant frequency after islanding occurs. The higher Q_f is, the quicker the system moves to the resonant frequency. Unfortunately, *RLC* loads with resonant frequencies close to the grid frequency or even matching this frequency are very common in the grid, as they are the result of compensating *RL*

inductive loads with capacitors in order to achieve a unity power factor.[1] That means that the islanding detection methods have to deal with these loads, in which a higher Q_f implies a higher tendency of the system to keep its frequency close to the grid frequency. As a consequence, a higher Q_f will tend to produce a bigger Non-Detection Zone and will difficult the methods to prevent the system from an islanding situation.

Standards and regulations indicate the load quality factor range for which the islanding prevention capability of the photovoltaic inverters has to be tested. As indicated before, *RLC* loads coming from *RL* loads that have been compensated are the most difficult ones. In these loads, the *RLC* quality factor Q_f is related to the *RL* power factor $cos\varphi_{RL}$ by means of:

$$Q_f = tg\left(\arccos\left[\cos\varphi_{RL}\right]\right) \tag{8}$$

A quality factor ranging from 0.5 to 2.5 is usually proposed to test the islanding detection methods.[1,5,27,29-31] A value of 2.5 corresponds to an *RLC* load whose *RL* part had a power factor of 0.37 before being compensated. This power factor is considered enough to include practically every load.[1]

III. THE FREQUENCY SHIFT ISLANDING DETECTION METHOD

III.1 The method and its parameters

The frequency shift method calculates the reference frequency for the inverter current as a function of both its instantaneous value and its variation with time.[1] Its implementation is usually carried out as follows:

$$f_{inv,n+1} = f_n + K_s \Delta f_n \tag{9}$$

where $f_{inv,n+1}$ is the reference frequency for the inverter current in the cycle $n+1$, f_n is the measured frequency in the cycle n, and K_s is the so-called frequency shift constant. Finally, Δf_n is the frequency variation detected in the cycle n, which is calculated as the difference between the actual frequency and the filtered frequency $f_{f,n}$:

$$\Delta f_n = f_n - f_{f,n} \tag{10}$$

The frequency shift constant K_s represents the first important parameter of the method. As long as the inverter remains connected to the mains, the frequency keeps constant and the instantaneous and filtered values are the same. When the mains is disconnected, the frequency moves depending on the characteristics of the load. From this moment, the instantaneous frequency tends to differ from the filtered value, which has *stored* the frequency of the mains, and the frequency shift method starts acting.

The filtered frequency $f_{f,n}$ is usually obtained by means of a low-pass filter. In spite of this filtering, transient situations can produce a high frequency shift thus injecting in the mains a distorted current when the grid is connected. In order to avoid it, the value of the frequency shift is limited as follows:

$$K_s \left|\Delta f_n\right| = K_s \left| f_n - f_{f,n} \right| \leq \Delta F_{\max} \tag{11}$$

In the last expression, ΔF_{max} is the so-called frequency shift limit, and represents the maximum allowed frequency variation. This is the second important parameter of the method.

Unlike the frequency filter, the design of K_s and ΔF_{max} is not easy and their choice will determine the detection capability of the method. This paper proposes a methodology to design these parameters in order to achieve the highest detection capability while minimizing the current distortion in normal condition.

III.2 Implementation on photovoltaic inverters

Figure 2 shows the inverter output current and voltage waveforms in a cycle n of any islanding situation in which the voltage is phase-lagged with respect to the current. The periods of the current and voltage waveforms are denoted as $T_{inv,n}$ and T_n, respectively. The frequency f_n is measured from the voltage waveform, i.e. it is the inverse of the period T_n. The current reference frequency $f_{inv,n}$ is calculated according to Equations (9) and (10). As the current is accurately controlled by the inverter, $T_{inv,n}$ is the inverse of $f_{inv,n}$. When the voltage finishes a

cycle, the current reference resumes to zero and starts a new cycle with the new reference frequency.

In case of islanding, the current and voltage waveforms differ in the phase-shift angle φ introduced by the load. This angle is defined as the phase-lag of the current with respect to the voltage (for Figure 2, φ is negative). In general, for a given frequency f, φ can be expressed as a function of R, L and C, as well as of the quality factor Q_f and the resonant frequency f_r:

$$\varphi = -arctg\left[R\left(2\pi fC - \frac{1}{2\pi fL}\right)\right] = -arctg\left[Q_f\left(\frac{f}{f_r} - \frac{f_r}{f}\right)\right] \tag{12}$$

Up to the resonant frequency, the angle φ stimulates the frequency shift and makes the frequency variation be greater than that one intended by the method. In fact, the system tends to the load resonant frequency even in the absence of the frequency shift method, as explained before. However, once the resonant frequency is reached, the load hinders the operation of the method and the angle φ tries to counteract the desired frequency variation slowing down the frequency shift. Depending on the load and the method parameters, the angle can even cancel the frequency shift causing the system to stay at the load resonant frequency.

Obviously, if the load resonant frequency is outside the limits of the frequency protection relays, these relays will be enough to detect islanding. Therefore, the frequency shift method has to be analysed for those frequencies that fall inside the trip limits of the relays.

Two options exist for the *direction* of the frequency shift after the grid disconnection. If the load resonant frequency is greater than the grid frequency, the system tends to increase its frequency. This situation will be called *increasing shift*. On the contrary, if the load resonant frequency is lower than the grid, the system frequency tends to decrease. This second situation will be called *decreasing shift*.

III.3 Photovoltaic inverter prototype used for simulations and experimental tests

As an example, the methodology proposed in this paper will be applied to a photovoltaic

inverter prototype. This prototype is basically the commercially available INGECON-SUN 2.5, from the company INGETEAM S.A. Its rated power is 2.5kW, and it is intended for 50Hz 230V grids. This inverter incorporates the frequency shift detection method as islanding detection active method, apart from voltage and frequency monitoring. The parameters of the method have been calculated by means of the proposed methodology, as described along the paper.

The photovoltaic inverter incorporates voltage and frequency protection relays with adjustable trip limits. For the tests developed along the paper, the voltage relay trip limits are set 10% over and 15% below the rated grid voltage, i.e., 253V and 195.5V. In turn, the frequency relay trip limits are set 2% over and below the rated grid frequency, that is, 51Hz and 49Hz.

IV. DESIGN OF THE FREQUENCY SHIFT CONSTANT K_S

When islanding occurs the system exhibits a natural tendency to move to the load resonant frequency. The frequency shift constant K_s has to be designed with the aim of counteracting this tendency in those situations in which the resonant frequency falls inside the protection relays limits. The analysis is made for an increasing shift. Concerning the decreasing frequency shift, it can be analysed in an analogous way with the same results as with the increasing shift.

In a cycle n+1 of an islanding situation, the inverter injects into the load a current with a frequency $f_{inv,n+1}$ that is calculated by means of Equation (9). As a consequence, the load introduces a phase-shift angle (φ, in radians) that can be expressed in terms of time (T_{ps}) as:

$$T_{ps} = \frac{\varphi}{2\pi} T_{inv,n+1} = \frac{\varphi}{2\pi f_{inv,n+1}} \tag{13}$$

When the voltage finishes the cycle, the frequency f_{n+1} is obtained as the inverse of the measured period T_{n+1}. As the phase-shift angle is defined as the phase-lag of the current with respect to the voltage, the values of T_{n+1}, $T_{inv,n+1}$ and T_{ps} are related as follows:

$$T_{n+1} = T_{inv,n+1} - T_{ps} = \frac{1}{f_{inv,n+1}} - \frac{\varphi}{2\pi f_{inv,n+1}} \tag{14}$$

With Equations (9) and (14), the measured frequency f_{n+1} can be expressed as:

$$f_{n+1} = \left(T_{n+1}\right)^{-1} = \left(\frac{1}{f_{inv,n+1}} - \frac{\varphi}{2\pi f_{inv,n+1}}\right)^{-1} = \left(\frac{1}{f_n + K_s \Delta f_n} - \frac{\varphi}{2\pi\left(f_n + K_s \Delta f_n\right)}\right)^{-1} \tag{15}$$

The main condition for K_s is to *keep* the frequency shift *after* the resonant frequency is reached. In principle, this condition implies that, for an increasing shift, the frequency in the cycle $n+1$ has to be greater than that one of the cycle n:

$$f_{n+1} = \left(\frac{1}{f_n + K_s \Delta f_n} - \frac{\varphi}{2\pi\left(f_n + K_s \Delta f_n\right)}\right)^{-1} > \left(\frac{1}{f_n}\right)^{-1} \tag{16}$$

And from this equation the following condition appears for K_s:

$$K_s > \frac{-\varphi f_n}{2\pi \Delta f_n} \tag{17}$$

As it was explained, up to the resonant frequency the load stimulates the frequency shift. After the resonant frequency, it is up to the islanding protection method to carry the frequency system outside the relay trip limits against the natural tendency of the load to its resonant frequency. Therefore, Equation (17) has to be analysed for frequencies greater than the load resonant frequency, and then the angle φ is negative according to Equation (12). Equation (17) can be thus better expressed as:

$$K_s > \frac{|\varphi| f_n}{2\pi \Delta f_n} \tag{18}$$

As the filtered frequency $f_{f,n}$ is constant and equal to the value of the grid frequency during the frequency shift, the term Δf_n is positive for an increasing frequency shift. Then, the condition expressed by Equation (18) provides, for a given quality factor Q_f and a resonant frequency f_r, the minimum positive value of K_s that counteracts the tendency to the load resonant frequency and guarantees an increasing frequency shift after the resonant frequency is reached.

However, the value of K_s has to be designed not only to counteract the tendency to the resonant frequency but also to move the system outside the protection relays trip limits in a maximum time, ensuring thus an islanding maximum length. This can be achieved by means of

guaranteeing that the period varies on each cycle a minimum time called the shift time (T_s). The condition for the upholding of the increasing frequency shift is then:

$$f_{n+1} = \left(\frac{1}{f_n + K_s \Delta f_n} - \frac{\varphi}{2\pi\left(f_n + K_s \Delta f_n\right)} \right)^{-1} \geq \left(\frac{1}{f_n} - T_s \right)^{-1} \tag{19}$$

As the angle φ is negative for an increasing shift, the condition for K_s is then given by:

$$K_s \geq f_n \frac{|\varphi| + 2\pi f_n T_s}{(1 - f_n T_s) 2\pi \Delta f_n} \tag{20}$$

The last expression depends on the frequency f_n and the load phase-shift angle φ. In turn, this angle depends on both the load resonant frequency f_r and the quality factor Q_f. Therefore, for a given quality factor, the minimum values of K_s are a function of both the actual frequency and the load resonant frequency.

However, Equation (20) can be still simplified. Let us denote K_{sm} as the minimum value of K_s given by Equation (20). The dependence of K_{sm} with the resonant frequency can be analysed by means of its partial derivative:

$$\frac{\partial K_{sm}}{\partial f_r} = -\frac{f_n}{(1 - f_n T_s) 2\pi \Delta f_n} \frac{Q_f}{1 + Q_f^2 \left(\frac{f_n}{f_r} - \frac{f_r}{f_n} \right)^2} \left(\frac{f_n}{f_r^2} + \frac{1}{f_n} \right) \tag{21}$$

As an increasing frequency shift has been supposed, the term Δf_n is positive. In addition, the term $1\text{-}f_n T_s$ is always positive due to the fact that, as it will be shown later, the values for T_s are required to be very small. Therefore the partial derivative of K_{sm} with respect to the resonant frequency is negative. As K_s has to be designed to cover the whole range of resonant frequencies, its calculation has to be done using the minimum value of the resonant frequency, which is the grid frequency f_g in the analysed frequency range. As a consequence, the calculation of K_s depends only on the measured frequency and the quality factor. The same conclusion is obtained when the decreasing frequency shift is analysed.

The previous analysis is now applied to the 50Hz 230V photovoltaic inverter prototype in order to design the value of K_s. The value of the filtered frequency $f_{f,n}$ during the islanding

detection process is the grid frequency, 50Hz. If the load is supposed to tend the system to increase its frequency, i.e. to cause an increasing shift, the period of the output voltage has to decrease 392μs (from 50Hz to 51Hz) in order to activate the protection relays and disconnect the inverter.

Most regulations for grid-connected photovoltaic systems specify the maximum islanding length by means of a maximum time or a maximum number of grid cycles. The worst condition for the islanding detection appears when the resonant frequency comes near to the grid frequency. In this situation, the frequency shift method has to take the frequency from the grid frequency to the upper relay trip limit, that is, to decrease the period a certain value. The shift time T_s can be calculated as the quotient of this value by the number of grid cycles required by the regulations. Islanding is a harmful situation, and regulations tend to establish very short detection lengths, which leads to very small values for T_s. Apart from regulations, it is clear that the quicker the island is detected the higher the performance of the protection method is. A detection time of 200ms (10 grid cycles) is usually considered as a very short time that guarantees personal safety and avoids interaction between the photovoltaic system and the grid reclosers.[1] If islanding is intended to be detected in less than 10 cycles, the period should decrease at least 39.2μs each cycle. This can be the value for T_s.

Equation (20) can now be evaluated to design K_s for the inverter prototype. Results are presented in Figure 3, which shows the minimum values of K_s as a function of the actual frequency f_n (increasing values from 50Hz) and the load quality factor Q_f (ranging from 0.5 to 2.5). The figure shows the minimum values of K_s that guarantee, for a measured frequency f_n, that the period decreases at least T_s. As expected, the values of K_s decrease with frequency. Therefore, once a value for K_s is chosen the frequency shift is guaranteed for measured frequencies equal or greater than the corresponding frequency. The values for K_s increase rapidly when frequencies get closer to the grid frequency (50Hz). Obviously, at 50Hz K_s is in theory infinite, that is, no value for K_s could make the system frequency move from this value.

The value for K_s has to be designed as a trade-off between the islanding capability and the distortion that the inverter could introduce in the grid during normal operation caused by frequency measurement errors and transients. Large values of K_s tend to achieve a high detection capability but also to increase the distortion. On the contrary, small values do not produce appreciable distortion when grid is connected but the frequency range in which detection is guaranteed decreases rapidly. According to Figure 3, a value of 5 for K_s, placed at the elbow of the curve, can be a good trade-off between both requirements for the inverter prototype. The graph shows that, with this value of K_s, detection is always guaranteed in less than 10 cycles for frequencies greater than 50.024Hz and quality factors up to 2.5.

Once K_s is chosen, there is a frequency range around the grid frequency in which the protection method will not guarantee the islanding detection in time. In the prototype, this range goes from 50Hz to 50.024Hz. An advantage of the proposed methodology is that the degree of protection against islanding can now be evaluated. The idea is to analyse how likely an islanding situation is to happen with this value for K_s, that is, how likely the measured frequencies between 50Hz and 50.024Hz are to be indefinitely. Just from the moment when a measured frequency is equal or greater than 50.024Hz the method starts acting and islanding is detected in less than 10 cycles. A frequency of 50.024Hz means a measured cycle period of 19.9904ms, i.e. only 9.6μs from the period of the grid voltage, 20ms, which is measured when the grid is connected. In other words, an accuracy of 99.95% is required in the measurement. In theory, loads with resonant frequencies between 50.024Hz and 50Hz could produce this situation. However, an error of such a small value (9.6μs) in the period measurement would be enough to start the frequency shift and detect the islanding situation in time. These errors are expectable and can come from electrical ripples, measurement noises, harmonic distortion, measurement digital procedures, etc.

Another idea of how much these values are small can be obtained in terms of the coupling in reactive power between the inverter and load. For the 2.5kW inverter prototype, Equations (2),

(4), (5), (6) and (7) show that a 50.024Hz resonant frequency when ΔP is zero corresponds to a 2.5 quality factor load that is consuming a reactive power ΔQ of around 12VAr, which means an extremely high degree of coupling between the photovoltaic inverter and the load.

In spite of these results, islanding detection could in theory be increased at its maximum level by means of programming a small disturbance of 9.6μs in the measured period that would act once each certain number of grid cycles. This would be enough to guarantee a total protection. Anyway, it has again to be remarked that no islanding situations can be realistically expected with period differences of 9.6μs.

The influence of the quality factor on the design of K_s is now discussed. As explained above, the need to achieve a high islanding detection capability restricts the K_s selection to frequencies close to 50Hz. In these frequencies, the influence of the load quality factor is considerably low. With a value of 5 for K_s, detection is guaranteed from 50.02Hz if the quality factor is 0.5, and from 50.024Hz if this factor is 2.5. That means a negligible difference in period of about 1.6μs, i.e. the detection capability is virtually identical. This is an important point to take into account in the design of K_s: the load quality factor does not have a substantial influence on it.

From a mathematical point of view, the influence of the quality factor becomes indeed negligible when Equation (20) is analysed for frequencies close to 50Hz. In these frequencies, the term $2\pi f_n T_s$ is quite greater than the phase-shift angle φ. If this angle is neglected, the influence of the quality factor on K_s disappears. For instance, at 50.02Hz, $2\pi f_n T_s$ reaches 12.3×10^{-3}rad, while a load with a resonant frequency of 50Hz and a quality factor of 2.5 introduces a phase-shift angle of 2×10^{-3}rad, which is six times lower. As a conclusion, due to the need of both a quick detection (low detection lengths, i.e. high values of T_s) and a high frequency detection range (frequencies very close to the grid frequency), the angle φ, and then the quality factor, has a reduced influence on the design of K_s. Based on this conclusion, Equation (20) can be simplified by eliminating the angle φ. In addition, the term $1-f_n T_s$ is practically 1. With these simplifications, Equation (20) can be approximated by:

$$K_s \geq \frac{f_n^2 T_s}{\Delta f_n} \tag{22}$$

This equation is more simple and practical than Equation (20), and can be used to design K_s instead.

V. DESIGN OF THE FREQUENCY SHIFT LIMIT ΔF_{MAX}

As it was explained in the previous section, K_s has to be designed as a trade-off between the detection capability and the amplification of small and constant distortions in the measured frequency. Even when K_s is designed in this way, the frequency shift ($K_s \Delta f_n$) has to be limited by ΔF_{max} in order to prevent strong transient disturbances in the measured frequency provoking a too high disturbing frequency shift. The drawback of limiting the frequency shift is that, on an islanding situation, some loads can introduce a phase-shift angle that cancels the intended frequency shift $K_s \Delta f_n$. The proposal is now to design ΔF_{max} as a function of the quality factor in such a way that frequency shift be always guaranteed for loads up to a minimum quality factor.

On each cycle, the period of the current waveform $T_{inv,n+1}$ is calculated with the aim of making the measured period of the voltage (T_n) vary a particular time (ΔT):

$$T_{inv,n+1} = T_n + \Delta T \tag{23}$$

This time variation ΔT can be expressed as an intended phase-shift angle φ_{int} of the current waveform with respect to the measured period of the voltage (T_n):

$$\varphi_{\text{int}} = \frac{2\pi}{T_n} \Delta T \tag{24}$$

From Equations (23) and (24), the expression of φ_{int} can be derived as follows:

$$\varphi_{\text{int}} = \frac{2\pi}{T_n}\left(T_{inv,n+1} - T_n\right) = 2\pi\left(\frac{T_{inv,n+1}}{T_n} - 1\right) = 2\pi\left(\frac{f_n}{f_{inv,n+1}} - 1\right) = 2\pi\left(\frac{f_n}{f_n + K_s \Delta f_n} - 1\right) \tag{25}$$

Both for an increasing and a decreasing shift, the loads that can cancel the intended phase-

shift angle φ_{int} are those loads which phase-shift angle φ is greater than φ_{int} in absolute values:

$$|\varphi| > |\varphi_{\text{int}}| \tag{26}$$

In case of an increasing frequency shift, $K_s\Delta f_n$ is positive and φ_{int} is negative. Besides, the load phase-shift angle φ is also negative as the voltage is phase lagged with respect to the current. Then, from the condition given by Equation (26):

$$-\varphi > -\varphi_{\text{int}} \quad \Rightarrow \quad tg(-\varphi) > tg(-\varphi_{\text{int}}) \tag{27}$$

The phase-shift angle of the load depends on the quality factor, the resonant frequency and the measured frequency, as it was shown in Equation (12). From this equation:

$$tg(-\varphi) = Q_f\left(\frac{f_n}{f_r} - \frac{f_r}{f_n}\right) \tag{28}$$

If the frequency shift $K_s\Delta f_n$ is limited to ΔF_{max}, the condition for the quality factors that can counteract the frequency shift can be obtained from Equations (25), (27) and (28):

$$Q_f\left(\frac{f_n}{f_r} - \frac{f_r}{f_n}\right) > tg\left(-2\pi\left(\frac{f_n}{f_n + \Delta F_{\max}} - 1\right)\right) \quad \Rightarrow \quad Q_f > \frac{tg\left(-2\pi\dfrac{f_n}{f_n + \Delta F_{\max}}\right)}{\dfrac{f_n}{f_r} - \dfrac{f_r}{f_n}} \tag{29}$$

If the minimum quality factor that fulfils Equation (29) is called $Q_{f,min}$, this equation indicates that, for a given ΔF_{max} and for any measured and resonant frequencies inside the protection relays trip limits, the frequency shift is guaranteed whenever the load quality factor is lower than $Q_{f,min}$. The dependence of $Q_{f,min}$ on the measured and resonant frequencies is now analysed. Concerning the resonant frequency, the dependence is given by:

$$\frac{\partial Q_{f,\min}}{\partial f_r} = tg\left(-2\pi\frac{f_n}{f_n + \Delta F_{\max}}\right)\frac{f_n\left(f_n^2 + f_r^2\right)}{\left(f_n^2 - f_r^2\right)^2} \tag{30}$$

The last expression is positive in case of an increasing frequency shift, where the measured frequencies f_n of interest for the islanding analysis are greater than the resonant frequency. Therefore, in order to calculate the minimum quality factor, a resonant frequency equal to the grid frequency has to be taken, as this is the lowest value in case of an increasing shift.

Concerning the dependence of $Q_{f,min}$ on the measured frequency, it is given by:

$$\frac{\partial Q_{f,\min}}{\partial f_n} = \frac{-\dfrac{1}{\cos^2\left(2\pi\dfrac{f_n}{f_n+\Delta F_{\max}}\right)}2\pi\dfrac{\Delta F_{\max}}{\left(f_n+\Delta F_{\max}\right)^2}\dfrac{f_n^2-f_r^2}{f_r f_n}-tg\left(-2\pi\dfrac{f_n}{f_n+\Delta F_{\max}}\right)\dfrac{f_n^2+f_r^2}{f_r f_n^2}}{\left(\dfrac{f_n^2-f_r^2}{f_r f_n}\right)^2} \quad (31)$$

The last expression is negative for an increasing frequency shift. As it could be expected, $Q_{f,min}$ increases as the measured frequency f_n decreases. Therefore, $Q_{f,min}$ has to be calculated for the highest measured frequency, which is the upper limit of the protection relay.

If the system tends to a decreasing frequency shift, the analysis for the minimum quality factor is similar as well as the results.

The minimum quality factors as a function of ΔF_{max} are now evaluated for the inverter prototype. Figure 4 shows the obtained results. For instance, if ΔF_{max} is chosen around 1.6Hz, islanding detection is guaranteed for load quality factors up to 5, a value even greater than the 0.5-2.5 range proposed by utilities and regulations to test the islanding detection methods. In addition, this value of ΔF_{max} limits the distortions effectively, as will be shown in the next section. For upper values and depending on the measured frequency and the load resonant frequency, the frequency shift might not be produced.

Finally, it is important to emphasize that the choice of ΔF_{max} has to be made with the aim of avoiding that load quality factors counteract the frequency shift intended by the method, while the islanding detection speed depends mainly on K_s.

VI. FREQUENCY DISTURBANCES WHEN THE GRID IS CONNECTED

When the grid is connected, its frequency is expected to be constant. In this situation, the measured frequency will be the same as the filtered frequency, and the frequency shift detection method will not act. However, frequency disturbances can appear coming from either the

measurement stage of the inverter or the grid itself. These disturbances will temporarily activate the frequency shift algorithm.

Compared to the time constant of the frequency filter, there can be short- and long-term disturbances. Short-term disturbances can appear as a consequence of momentary grid disturbances, measurement errors, etc. Long-term frequency disturbances can be caused, for instance, by the connection or disconnection of large loads to the grid. While the first ones do not affect the value of the filtered frequency, long-term disturbances imply a change of the filtered frequency to the new value of the frequency grid. Anyway, it is important to point out that in both situations the interaction with the frequency shift method is transient by nature. This is obvious for short-term disturbances. In the case of long-term disturbances, the interaction appears only during the time the filtered frequency reaches the value of the measured frequency.

The effect of a disturbance in the measured frequency is shown in Figure 5. In this figure, the measured frequency is slightly higher than the grid frequency. Therefore, the current generated by the inverter is not in phase with the output voltage. At the end of each cycle, the inverter detects the output voltage zero crossing and makes the current start a new cycle. As a consequence, during the time of the disturbance the inverter injects temporarily into the grid a harmonic distorted current with a dc-component. Figure 6 shows the relationship between the magnitude of both effects and the product $K_s\Delta f_n$. In this figure, the current dc-component, given as a percentage of the inverter rated rms-current, and the Total Harmonic Distortion THD are calculated as a function of $K_s\Delta f_n$. Both graphs help to establish the upper limits for the values of K_s and ΔF_{max} as a function of the expected disturbances in the measured frequency, which depend mainly on the inverter implementation and the grid characteristics.

For the photovoltaic inverter prototype, K_s was proposed to be 5. The variations in frequency of the mains and the measurement errors are usually very small. As an example, if disturbances in the frequency are expected to be less than 0.2Hz ($K_s\Delta f_n$ equals 1), it appears from Figure 6 that the current THD during the time of the disturbance will not be greater than 4% and the dc-

component will be around 0.0025% of the rated rms-current. Higher values for K_s will decrease progressively the quality of the current, while they will not achieve an important improvement in the detection capability. Concerning ΔF_{max}, a value of 1.6Hz was chosen in the previous section for the inverter prototype. According to Figure 6, if $K_s \Delta f_n$ is limited to 1.6Hz, THD will never exceed 6% during the time of the disturbance and the dc-component will be always lower than 0.005%.

As a conclusion, Figure 6 should be used together with Figures 3 and 4 in order to design K_s and ΔF_{max}.

VII. ANALYSIS OF THE ISLANDING DETECTION CAPABILITY

VII.1 The simulation procedure

This section analyses by simulation the islanding detection capability of the method once designed with the proposed methodology. The experimental results are shown in the next section.

The simulations are based on MATLAB/SIMULINK and try to represent as far as possible the real operation of the complete system, including the photovoltaic generator, the inverter prototype, the grid and the *RLC* load. The simulation of the inverter includes aspects such as the switching and dead times of the power semiconductors (IGBTs), the output current and power factor control loops, the output filtering stage, etc. The inverter is supplying its rated power, i.e. 2.5kW. The frequency shift method is digitally implemented on it with the proposed parameters K_s=5 and ΔF_{max}=1.6Hz.

The analysis is carried out by means of the islanding maps, where ΔP and ΔQ are the horizontal and vertical axes, respectively.[2,5] A grid is defined in the maps, and the system is simulated at each point of the grid by means of adjusting *R*, *L* and *C* according to Equations (5), (7) and (9). The following codes are used for the maps:

- • (dot): islanding not detected
- 1: detection by the over voltage relay (voltage rms-value greater than 253V)
- 2: detection by the under voltage relay (voltage rms-value lower than 195.5V)
- 3: detection by the over frequency relay (frequency greater than 51Hz)
- 4: detection by the under frequency relay (frequency lower than 49Hz)

It has to be pointed out that in some points of the maps the detection is achieved both by a frequency and a voltage relay. In these situations, only the number corresponding to the voltage relay is depicted in the map. Therefore, detection by the voltage relays appears overrated, although this is not important for the analysis of the detection capability.

VII.2 Islanding Maps

In order to show the islanding detection capability of the frequency shift method, these maps are calculated in two situations. Firstly, the islanding maps are calculated when only voltage and frequency monitoring detection methods are implemented in the inverter. Results are shown in Figure 7, where the maps are obtained for two load quality factors: 0.5 and 2.5. As it is characteristic of these passive methods, both maps exhibit an important NDZ. In addition, the NDZ increases when the quality factor is 2.5, as expected. The NDZ of the maps do not have exactly the typical trapezium shape. This is due to the fact that the control loops, the switching of the power semiconductors, the output filter, etc., can generate in the simulated output voltage and frequency small distortions and oscillations that affect the activation of the relays in those points placed in the border between the detection and non-detection zones. In addition, the islanding maps are slightly shifted up due to the small reactive power generated by the inverter, about 35VAr, corresponding to a power factor of 0.999.

When the frequency shift islanding detection method is also implemented in the inverter, no NDZ appears in the islanding maps, as shown in Figure 8, which presents the maps for both quality factors, 0.5 and 2.5. In order to try to find non-detection points, additional maps were

simulated with narrower grid steps up to 10W and 2VAr, but no NDZ was obtained. An example is presented in Figure 9, which shows the simulation results for a particular point, corresponding to ΔP=-50W and ΔQ=38VAr. This point is just on the border between the over and under frequency detections (numbers 3 and 4). In this simulation, the mains is disconnected at cycle 30 (t=0.6s) and islanding is detected in cycle 34. Simulation results show how the measured, filtered and inverter frequencies move outside the relays trip limits after the mains is disconnected.

VII.3 Influence of K_s and ΔF_{max} on the detection capability

In order to test the influence of K_s on the islanding detection capability, this parameter is reduced with the aim of finding non-detection points. Reductions up to K_s=2 could not find non-detection points even when the grid was reduced up to 5VAr. However, for K_s=1 and Q_f=2.5, some non-detection points appear. An example is the point corresponding to ΔP=0W and ΔQ=91VAr, which results are shown in Figure 10. The system remains at the islanding situation after some oscillations in the frequency.

Concerning ΔF_{max}, its value was proposed to be chosen as a function of the maximum quality factor for which detection has to be completely guaranteed. Once ΔF_{max} is selected according to a particular quality factor, islanding detection is not always guaranteed for loads with higher quality factors. In these cases, detection depends on the measured frequency and the load resonant frequency. For the inverter prototype, Figure 4 showed that with the design value of ΔF_{max} (1.6Hz) detection is not completely guaranteed for quality factors greater than 5. In order to validate the proposed methodology for the design of ΔF_{max}, the left map of Figure 11 shows the islanding map for a quality factor of 7 and the design values for K_s and ΔF_{max} (5 and 1.6Hz). As predicted by the analysis of ΔF_{max}, now it does indeed exist a NDZ. If the method is intended to completely guarantee islanding detection for quality factors up to 7, ΔF_{max} has to be increased. According to Figure 4, a value of 2.5Hz for ΔF_{max} should be enough to cancel the

NDZ. The new islanding map with ΔF_{max}=2.5Hz is shown in the right map of Figure 11. As predicted, even though the grid has been considerably narrowed, no NDZ is now found.

VIII. EXPERIMENTAL TESTING OF THE ISLANDING DETECTION CAPABILITY

The design methodology for the frequency shift islanding detection method is now validated through experimental tests on the commercial inverter prototype described in Section III.3. The inverter incorporates the method with the design values (K_s=5 and ΔF_{max}=1.6Hz).

For the experimental set-up, a 50Hz 230V grid was used, and a photovoltaic simulator supplied the inverter at a constant 2.5kW dc power. The experimental tests were carried out by means of adjusting the *RLC* load in order to both achieve a 2.5 quality factor and make the real and reactive powers consumed by the load match the real and reactive powers delivered by the inverter. In this situation, ΔP and ΔQ are practically zero, and so is the current coming from the mains before islanding. This is the most difficult situation for the islanding to be detected, as the disconnection of the grid will hardly affect the behaviour of the power section. Therefore, this is an appropriate test to validate the detection capability of the method.

Two tests are carried out. In the first one, only the voltage and frequency monitoring methods are included. In the second one, the frequency shift detection method is also incorporated. In the figures shown below, v_{inv} and i_{inv} denote the inverter output voltage and current, respectively, and i_{grid} denotes the current coming from the mains. In addition, V and F denote the rms-value and frequency of the inverter output voltage v_{inv}.

Figure 12 shows the moment when islanding appears. As the load has been tuned to match the inverter real and reactive powers, the current from the mains (i_{grid}) is, before islanding, practically zero except for the noise. Then, on a given moment the mains is disconnected, i_{grid} goes zero and islanding appears. This is the initial situation for both tests.

Figure 13 shows the results for the first test, in which the frequency shift detection is not implemented. As expected from the islanding maps of Figure 7, the islanding situation is not detected and the inverter remains supplying the load due to the power coupling between load and inverter. The voltage rms-value (V) and frequency (F) are measured with a Yokogawa WT1600 Digital Power Meter, which is programmed to take values once per second. When islanding appears, the voltage rms-value V moves from 219.5V to 213V and the frequency F decreases from 50.04Hz to 49.71Hz. After that, the values remain stationary inside the trip limits and the protection relays do not activate.

When the frequency shift detection method is implemented in the inverter, and in the same conditions as the previous test, islanding is detected, as shown in Figure 14. The figure shows the evolution of the last cycles of the islanding situation. Some cycles after the grid is disconnected, the frequency goes outside the trip limits and the islanding is detected. In this moment, the inverter stops supplying the load and the output voltage and current (v_{inv} and i_{inv}) go zero. These results validate the proposed methodology to design the method and detect islanding even when the real and reactive powers supplied by the photovoltaic inverter match the real and reactive powers consumed by the load.

IX. CONCLUSIONS

Islanding is an undesirable behaviour of a grid-connected photovoltaic system in which the photovoltaic inverter continues supplying the load that remains in the same power section after the mains is disconnected. National and international regulations demand effective protection against this situation. The Sandia Frequency Shift method is one of the most important active methods and exhibits several advantages apart from its high detection capability. It does not need to introduce a periodic disturbance to detect islanding like the active frequency drift and impedance measurement methods, and it does not require real power variation like the voltage

shift method.

The frequency shift method implements a positive feedback of the measured frequency. When islanding appears, the frequency changes and the method tries to move the frequency outside the protection relay trip limits by means of modifying the frequency of the inverter current in the same direction.

The detection capability of the method depends on both the parameters of the method and the load characteristics. In this paper, a new methodology has been proposed to design the two main parameters of the method as a trade-off between the detection capability and the distortion that the method can introduce on the mains when transitory frequency changes appear. The detection capability is evaluated as a function of the parameters of the load, mainly the quality factor and the resonant frequency.

The proposed design methodology is applied to a commercial photovoltaic inverter prototype. This inverter implements the frequency shift method and its parameters are designed along the paper. Simulation and experimental results prove the ability of the proposed methodology to design the parameters of the method and achieve the highest detection capability. From the analysis it can be concluded that when the parameters are designed according to the proposed methodology the islanding condition is virtually impossible to happen while the interaction with the grid during normal operation is minimized.

REFERENCES

1. Stevens J, Bonn R, Ginn J, Gonzalez S, Kern G, Development and testing of an approach to anti-islanding in utility-interconnected photovoltaic systems, *Sandia National Laboratories*, USA, August 2000.
2. Ropp ME, Begovic M, Rohatgi A, Prevention of islanding in grid-connected photovoltaic systems, *Progress in Photovoltaics: Research and Applications* 1999; **7**: 39-59.
3. Cullen N, Risk analysis of islanding, *Proceedings of the workshop Impacts of PV Penetration In Distribution Networks Workshop*, IEA Task V, Arnhem, The Netherlands, 2002.
4. Wills R, Universal interconnection technology, *U.S. Department of Energy Universal Interconnection Technology Workshop*, Chicago, 2002.
5. Woyte A, De Brabandere K, Van Dommelen D, Belmans R, Nijs J, International harmonization of grid connection guidelines: adequate requirements for the prevention of unintentional islanding, *Progress in Photovoltaics: Research and Applications* 2003; **11**: 407-424.
6. Begovic M, Ropp ME, Rohatgi A, Pregelj A, Determining the sufficiency of standard protective relaying for islanding prevention in grid-connected PV systems, *2nd World Conference and Exhibition on Photovoltaic Solar Energy Conversion*, Vienna, Austria, 1998.
7. Verhoeven B, Probability of islanding in utility networks due to grid connected photovoltaic power systems, *IEA Report PVPS T5-07: 2002*, 2002.
8. Kobayashi H, Takigawa K, Statistical evaluation of optimum islanding preventing method for utility interactive small scale dispersed PV Systems, *IEEE Photovoltaic Specialists Conference*, Hawaii, 1994; 1085-1088.
9. Kobayashi H, Takigawa K, Hashimoto E, Kitamura A, Matsuda H, Method for preventing islanding phenomenon on utility grid with a number of small scale PV systems, *IEEE Photovoltaic Specialists Conference*, Las Vegas, Nevada, 1991; 695-700.
10. Ropp ME, Design issues for grid-connected photovoltaic systems, *Ph. D. dissertation, Georgia Institute of Technology*, Atlanta, USA, 1998.
11. Ropp ME, Begovic M, Rohatgi A, Analysis and performance assessment of the active frequency drift method of islanding prevention, *IEEE Transactions on Energy Conversion* 1999; **14**(3): 810-

816.

12. Hung GK, Chang CC, Chen CL, Automatic phase-shift method for islanding detection of grid-connected photovoltaic inverters, *IEEE Transactions on Energy Conversion* 2003; **18**(1): 169-173.

13. Kern GA, SUNSINE300, utility interactive AC module anti-islanding test results, *IEEE 26th Photovoltaic Specialists Conference*, Anaheim, California, 1997; 1265-1268.

14. Ropp ME, Begovic M, Rohatgi A, Kern GA, Bonn RH, Gonzalez S, Determining the relative effectiveness of islanding detection methods using phase criteria and nondetection zones, *IEEE Transactions on Energy Conversion* 2000; **15**(3): 290-296.

15. Woyte A, Belmans R, Nijs J, Testing the islanding protection function of photovoltaic inverters, *IEEE Transactions on Energy Conversion* 2003; **18**(1): 157-162.

16. Onions PA, Smith GA, Anti-islanding protection of grid connected PV inverters, *34th Universities Power Engineering Conference UPEC'99*, Leicester, United Kingdom, 1999; 378-382.

17. Schulz D, Hanitsch R, Proposals for an international islanding detection standard, *World Renewable Energy Congress*, Cologne, Germany, 2002.

18. Bower W, Ropp M, Evaluation of islanding detection methods for photovoltaic utility-interactive power systems, *IEA Report PVPS T5-09: 2002*, 2002.

19. Verhoeven B, Utility aspects of grid connected photovoltaic power systems, *IEA Report PVPS T5-01: 1998*, 1998.

20. Köln K, Grabitz A, Kremer P, Kress B, Five years of ENS (MDS) islanding protection – What could be the next steps?, *17th European Photovoltaic Solar Energy Conference and Exhibition*, Munich, Germany, 2001.

21. Yuyama S, Ichinose T, Kimoto K, Itami T, Ambo T, Okado C, Nakajima K, Hojo S, Shinohara H, Ioka S, Kuniyoshi M, A high speed frequency shift method as a protection for islanding phenomena of utility interactive PV systems, *Solar Energy Materials and Solar Cells* 1994; **35**(1-4): 477-486.

22. Okado C, Kimoto K, Shinohara H, Ichinose T, A novel islanding protection system for photovoltaic inverters, *Electrical Engineering in Japan* 1995; **115**(4): 60-70.

23. Okado C, Protection device for stopping operation of an inverter, *US Patent no. 5493485*, December 29, 1993.

24. Smith GA, Onions PA, Infield DG, Predicting islanding operation of grid connected PV Inverters, *IEE Proceedings Electric Power Applications* 2000; **147**(1): 15-20.

25. Kern GA, Bonn RH, Ginn J, Gonzalez S, Results of Sandia National Laboratories grid-tied inverter testing, Sandia National Laboratories, *2nd World Conference and Exhibition on Photovoltaic Solar Energy Conversion*, Vienna, Austria, 1998.

26. Huang SJ, Pai FS, Design and operation of grid-connected photovoltaic system with power-factor control and active islanding detection, *IEE Proceedings on Generation, Transmission and Distribution* 2001; **148**(3): 243-250.

27. IEEE Std 929-2000, IEEE Recommended practice for utility interface of photovoltaic (PV) systems, *Institute of Electrical and Electronics Engineers*, New York, USA, 2000.

28. Automatic disconnecting facility for photovoltaic installation with a rated output ≤ 4.6 kVA and a single-phase parallel feed by means of an inverter into the public low-voltage mains, *German National Standard DIN VDE 0126*, 1999.

29. UL 1741, UL Standard for safety for static converters and charge controllers for use in photovoltaic power systems, *Underwriters Laboratories Inc.*, Northbrook, USA, 1999, Revised Jan. 2001.

30. IEEE Draft Standard for Interconnecting Distributed Resources with Electric Power Systems, IEEE P1547/D07, *Institute of Electrical and Electronics Engineers*, 2001.

31. Recommendation for the connection of small-scale embedded generators (up to 16A per phase) in parallel with public low-voltage distribution networks, *United Kingdom Engineering Recommendations G83*, 2003.

FIGURE 1

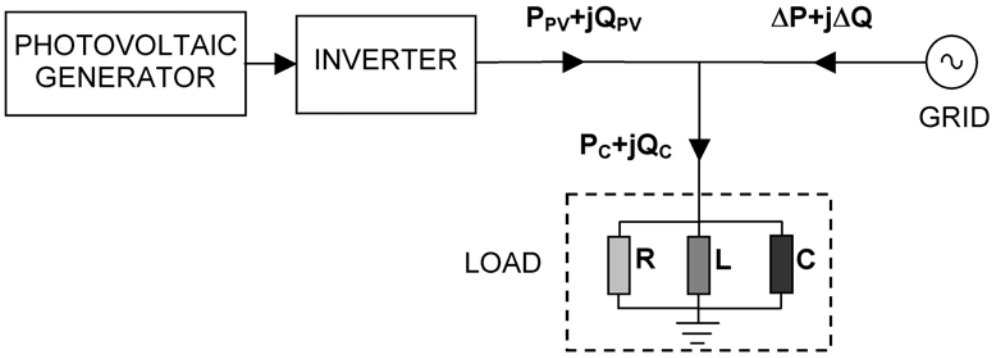

Figure 1. Photovoltaic system, load and grid connection before islanding: definition of ΔP and ΔQ.

FIGURE 2

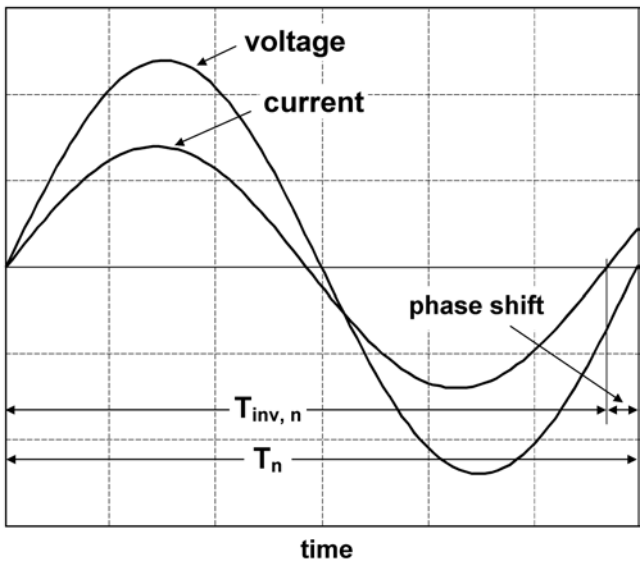

Figure 2. Inverter output current and voltage on a cycle *n* of an islanding situation.

FIGURE 3

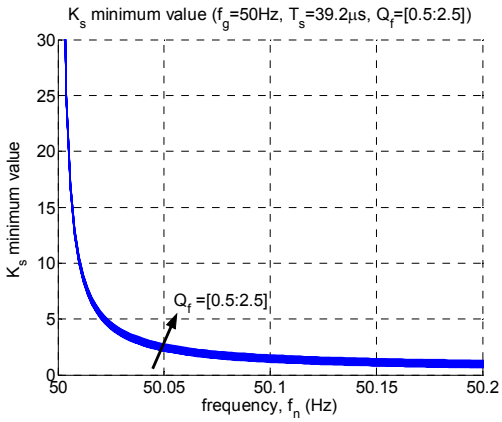

Figure 3. Minimum values of K_s as a function of the actual frequency f_n and the load quality factor Q_f for an increasing frequency shift.

FIGURE 4

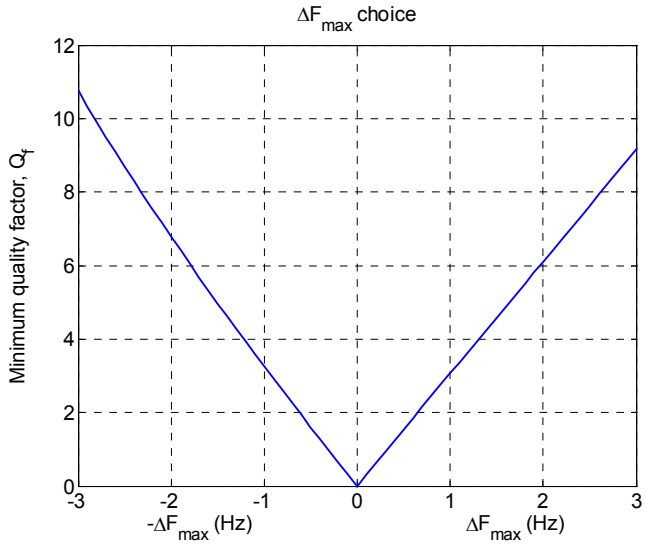

Figure 4. Design of ΔF_{max}. Load minimum quality factors above which islanding is not guaranteed.

FIGURE 5

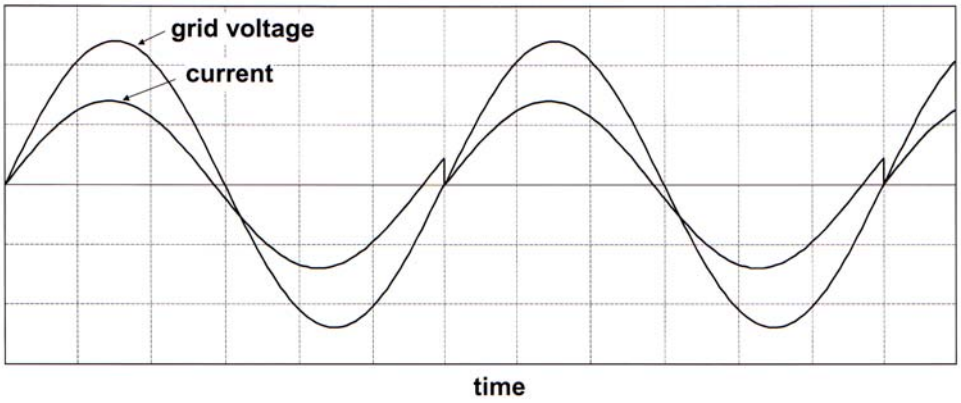

Figure 5. Influence of a frequency disturbance on the inverter current when grid is connected.

FIGURE 6

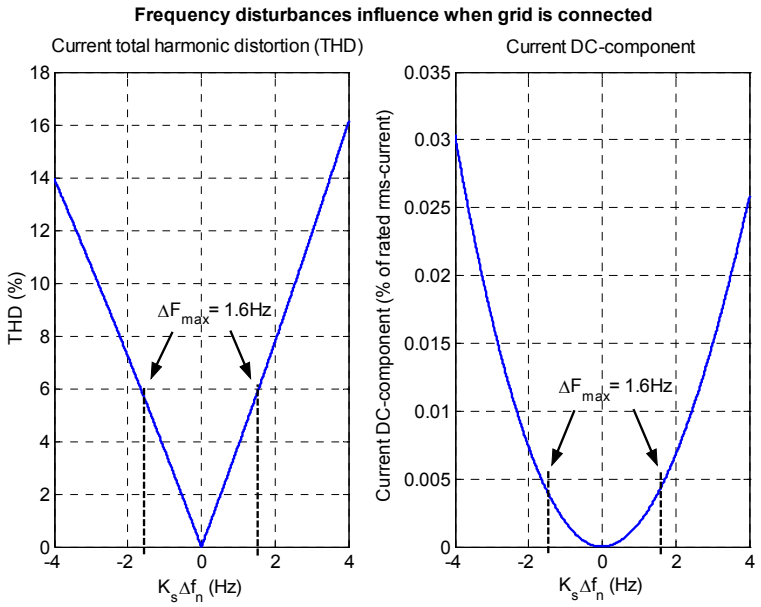

Figure 6. Influence of a temporary frequency disturbance on the current (dc-component and Total Harmonic Distortion) as a function of $K_s\Delta f_n$.

FIGURE 7

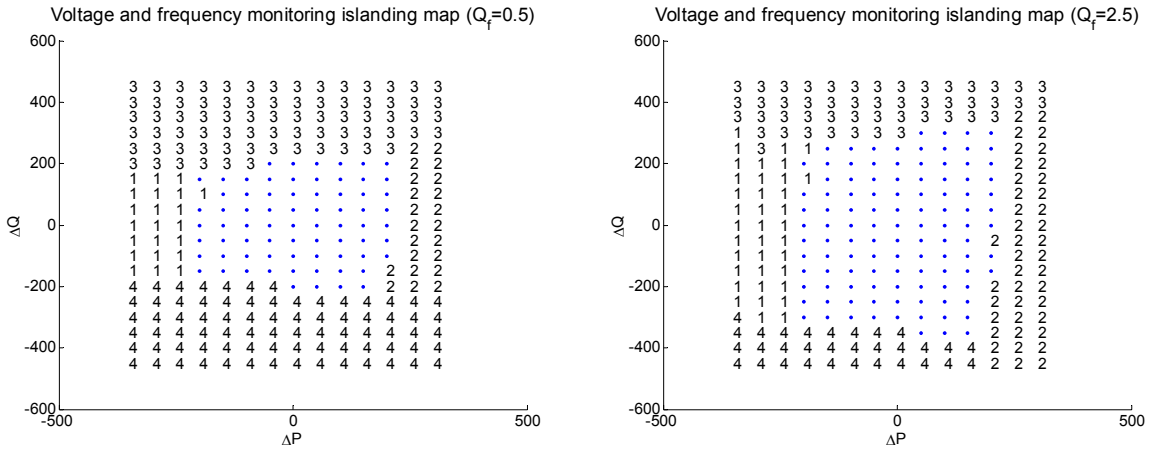

Figure 7. Islanding maps when only voltage and frequency monitoring are implemented, for Q_f=0.5 (left), and Q_f=2.5 (right).

FIGURE 8

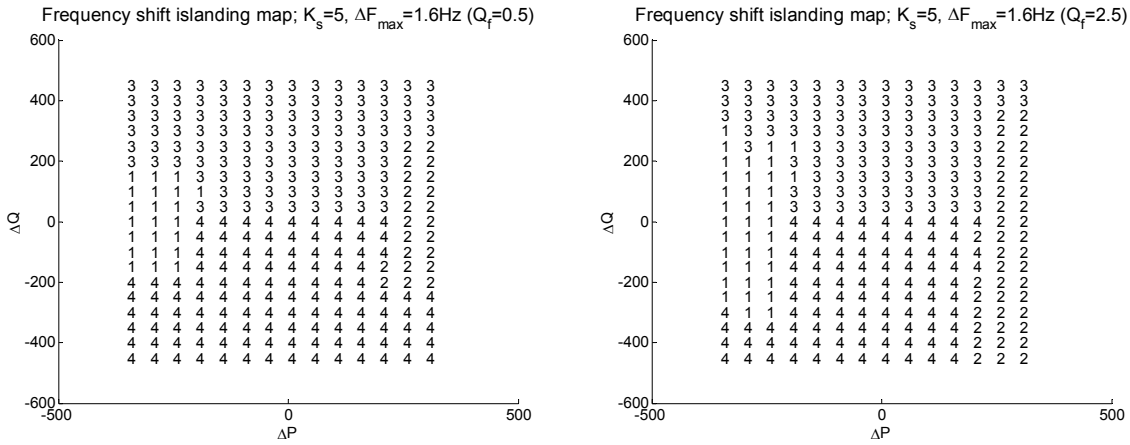

Figure 8. Islanding maps for Q_f=0.5 (left) and Q_f=2.5 (right) when the frequency shift method, designed with the proposed methodology (K_s=5, ΔF_{max}=1.6Hz), is implemented on the inverter prototype.

FIGURE 9

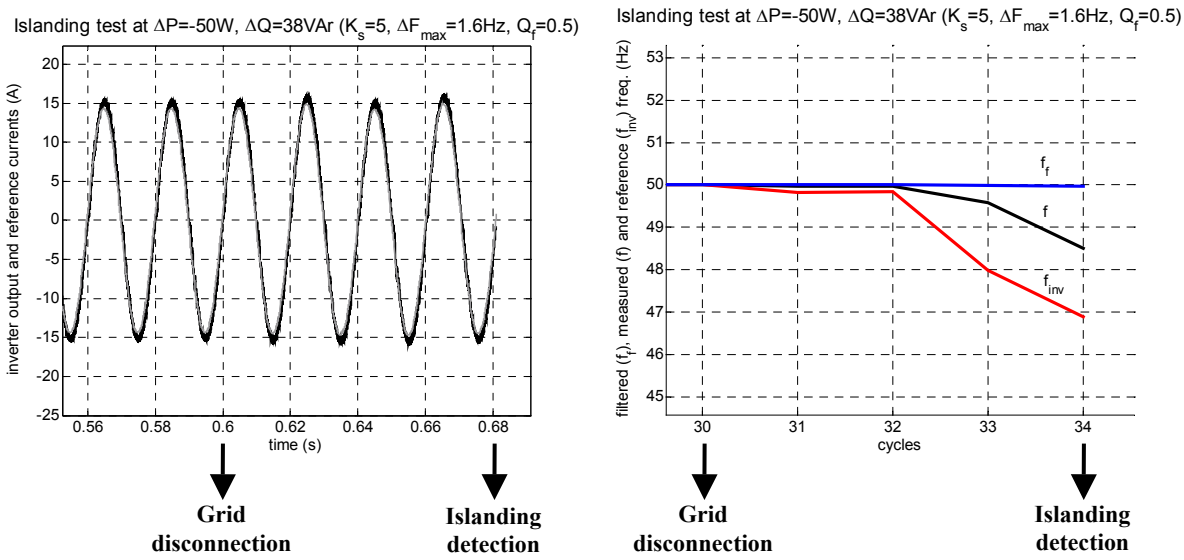

Figure 9. Islanding test at ΔP=-50W and ΔQ=38VAr, with Q_f=0.5 (K_s=5 and ΔF_{max}=1.6Hz). The grid is disconnected at cycle 30 (t=0.6s) and the islanding situation is detected at cycle 34 (t=0.681s).

FIGURE 10

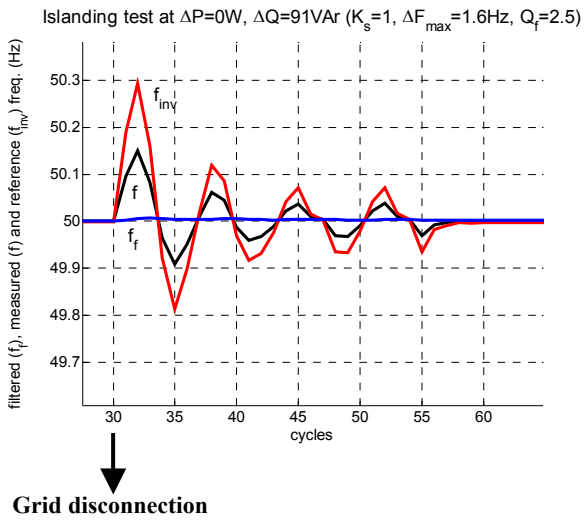

Figure 10. Islanding test at ΔP=0W and ΔQ=91VAr. The frequency shift method is implemented but the value of K_s decreases to 1, while ΔF_{max} remains at 1.6Hz. The load quality factor Q_f is 2.5. The grid is disconnected at cycle 30 and the islanding situation is not detected.

FIGURE 11

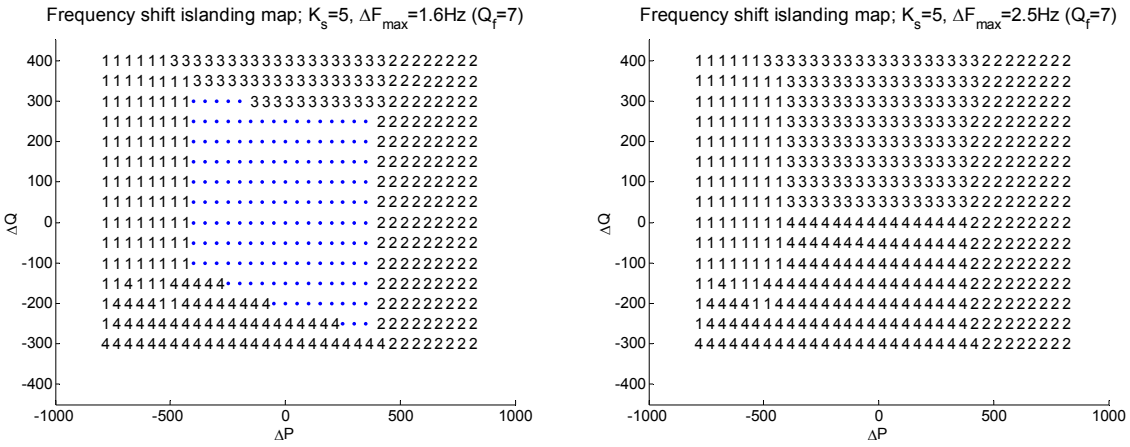

Figure 11. Islanding maps for ΔF_{max}=1.6Hz (left) and ΔF_{max}=2.5Hz (right) when Q_f=7.

FIGURE 12

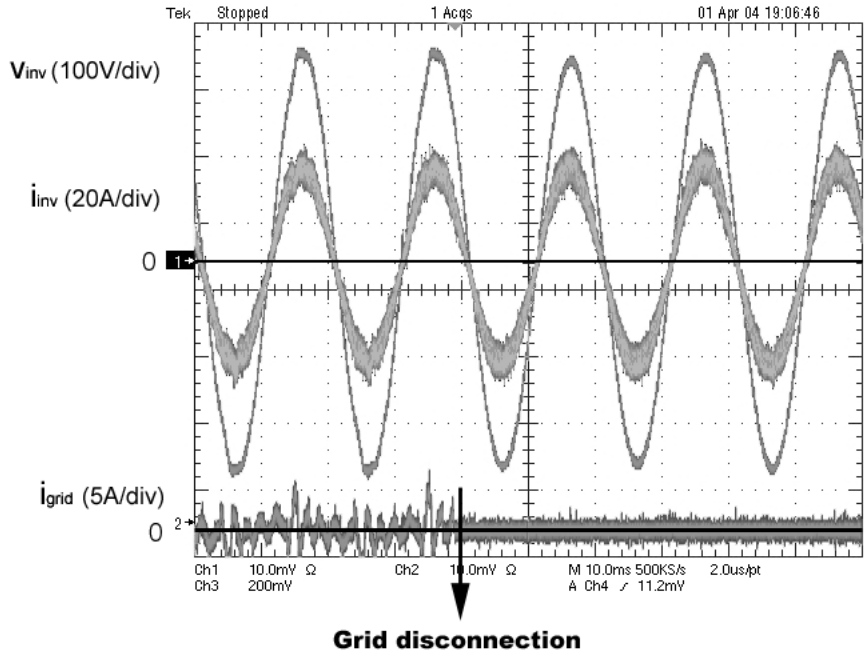

Figure 12. Inverter output voltage (v_{inv}, 100V/div) and current (i_{inv}, 20A/div), and mains current (i_{grid}, 5A/div), when grid is suddenly disconnected and islanding appears.

FIGURE 13

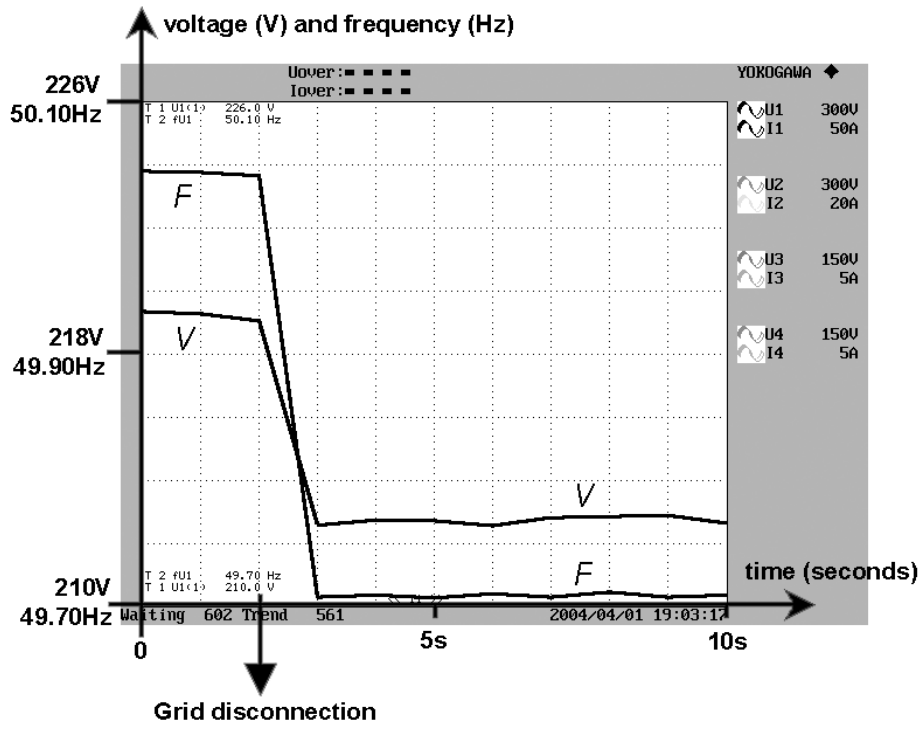

Figure 13. Islanding situation when the inverter includes only the voltage and frequency monitoring methods. Output rms-voltage (*V*) and frequency (*F*) before and after the grid is disconnected measured by a Yokogawa WT1600 Digital Power Meter that takes values once per second.

FIGURE 14

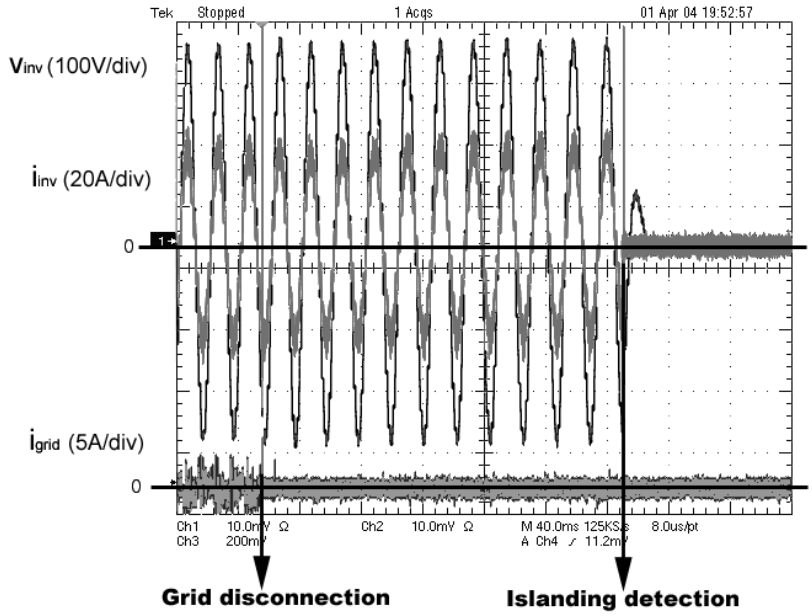

Figure 14. Islanding detection when the frequency shift method is incorporated to the inverter prototype. Inverter output voltage (v_{inv}, 100V/div) and current (i_{inv}, 20A/div), and mains current (i_{grid}, 5A/div).